



Chiral monomer template for designing Low-Driving-Field blue phase liquid crystals

Srinivas Pagidi^{a,d}, Ramesh Manda^{b,*}, Sujaya Kumar Vishwanath^c, Moon-Young Choi^a, Mohsin Hassan Saeed^a, Surajit Dhara^b, Jun-Hee Na^{a,*}

^a Department of Electrical, Electronics and Communication Engineering Education and Department of Convergence System Engineering, Chungnam National University, Yuseong-gu, Daejeon 34134, Republic of Korea

^b School of Physics, University of Hyderabad, Gachibowli, Hyderabad, Telangana 500046, India

^c Center for Nano Science and Engineering, Indian Institute of Science, Bangalore, Karnataka 560012, India

^d Department of Electrical & Electronic Engineering, Southern University of Science and Technology, Xueyuan Road 1088, Nanshan District, Shenzhen, Guangdong 518055, China

ARTICLE INFO

Keywords:

Liquid Crystal
Blue Phase Liquid Crystal
Chiral Monomer template
Kerr effect

ABSTRACT

Blue phase liquid crystals (BPLC) are known to be useful for various non-trivial applications due to their nanoscale self-assembled cubic crystalline structures. Even though the BPLC exhibits an efficient optically isotropic phase due to the double helical confinement of liquid crystal (LC) molecules within a few hundred-nanometer range, this hinders the orientation of LC molecules along the applied field direction. Consequently, the BPLC demands larger driving fields to operate, degrading the device's performance in real-world applications. In this context, we provide a chiral monomer template for BPLC that decreases the driving field by 52 % while the electro-optical responses remain unaffected. Furthermore, our approach provides higher thermal stability, with a broader BPLC phase range (42 °C), including near ambient temperature. As this approach potentially overcomes the fundamental challenges of BPLC, the proposed system could be useful for next-generation display devices.

1. Introduction

Owing to the inherent nanoscale self-assembly, the blue phase (BP) liquid crystals (LC) are suitable for many non-trivial applications such as in highly efficient sensors, field-sequential LC displays, lenses, lasers, phase gratings, optical elements, smart photonic devices, etc. [1–5]. The BPLC inherently comprises double twisted cylinders (DTCs), formed by twisting LC molecules (-45° on one side to $+45^\circ$ on another) across its diameter. It creates a cubic lattice with a lattice constant in the visible wavelength range. The DTCs are self-assembled into three hierarchical BP phases, namely BP I (Body-Centered Cubic), BP II (Simple Cubic), and BP III (Amorphous), based on their cubic symmetry. Owing to the cubic symmetry, it exhibits several unconventional properties, such as optically isotropic phase and sub-millisecond electro-optical response time. It also offers devices that are alignment layer-free and have wide viewing angles [6–10]. These self-assembled complex structures with cubic symmetry exhibit photonic band gaps capable of 3-dimensional localization of light. Especially, BP I and II are considered soft

photonic crystals as they allow the manipulation of structures by various external stimuli, such as light, thermal, electric, and magnetic fields. Such a structural manipulation opens new pathways to narrow the optical bandwidth and band gaps for adaptive structural coloration and 3-dimensional photonic effects [11,12]. Unfortunately, the topological line defects (disclinations) evolve between the DTCs, as the cylindrical structures cannot fill the 3-dimensional space; hence they act as singular points to destabilize the BP phase. So far, several techniques have been proposed to overcome the aforementioned challenges. For instance, a polymer-stabilized blue phase liquid crystal (PS-BPLC) is a system that overcomes low thermal stability [13–17]. The dispersed monomers selectively fill inside the disclinations and reduce the free energy of the BP upon polymerization. Thus, the BPLC becomes stable over a long temperature range. Similarly, an ultra-stable BP system was proposed using the molecular synergistic self-assembly of molecules with distinct configurations, which is a low-molecular-weight BP system with the widest temperature range (over 130 °C) [16]. Novel materials with engineered structures, such as bend-core [18,19], hydrogen-bonded

* Corresponding authors.

E-mail addresses: manda_rff@uohyd.ac.in (R. Manda), junhee.na@cnu.ac.kr (J.-H. Na.).

<https://doi.org/10.1016/j.molliq.2024.124311>

Received 16 October 2023; Received in revised form 5 February 2024; Accepted 20 February 2024

Available online 25 February 2024

0167-7322/© 2024 Elsevier B.V. All rights reserved.

[20], biaxial materials like U-shaped, T-shaped [21], nanoparticles, and quantum dots [22,23], have also been proven to be potentially valuable to overcome the thermal stability issue. However, these systems introduce new challenges; for example, the PS-BPLC technique requires a high-driving electric field to switch the phase and unwanted photonic effects. Despite several efforts to overcome these issues [24–26], the fabrication of the ideal BP, which is stable over a wide temperature range with optimal electro-optical properties, remains a critical challenge. Recent advances in polymer stabilization techniques require the use of chiral and mesogenic monomers for phase stabilization, which have shown great potential for overcoming both of these challenges. In such systems, a polymer network is formed inside the disclination lines and the DTC without disturbing the local ordering of LC molecules. It ensures phase stability for a more comprehensive temperature range while reducing the driving field and maintaining higher mechanical stability [4,27–31]. However, further phase stability optimization with a reduced driving field is highly desired.

The templated BPLC has recently proven to be a promising approach to addressing high driving fields and low thermal stability issues [32–36]. After LC and chiral dopant molecules extraction, a PS-BPLC serves as a hard template for achiral LC to reproduce the BP in this approach. The highly twisted reconfiguration capability of achiral LC in this template originates from the strong surface memorized anchoring rather than the properties of the bulk materials. Furthermore, owing to the polymer-directed LC molecular orientation, which possesses no significant frustration, the phase gains high thermal stability. Taking advantage of this polymer-directed templated BP, several electro-optical devices, hyper-reflective films, tunable band gaps, and mirrorless lasers have been demonstrated [37–40]. Not limited to BPLC, this technique has been implemented in several systems for enriching photonic effects, sensing, and display applications [41–44]. Although this approach significantly reduces the required driving field to $\sim 8 \text{ V}/\mu\text{m}$ [35,45], it is still higher for conventional driving circuits, such as thin-film-transistors (TFTs). Therefore, further reduction in the driving field is highly desirable from the perspective of future smart devices.

In this paper, we demonstrated a templated BPLC fabricated by a novel polymerization technique that has reduced the driving field and enhanced thermal stability compared to previously reported values [29,35]. We found that the chiral monomer stabilized BPLC (CMS-BPLC), which provides structural stability to DTC, can act as an effective template for achiral nematic LC to reproduce BPLC. Refilling the achiral nematic LC into this CMS-BPLC template named T-BPLC, we achieved a broader BP phase of nearly 42°C , including near room temperature. The T-BPLC developed by us reduces the operating and the threshold fields by more than half while keeping other electro-optical properties unaffected.

2. Experimental procedure

2.1. Materials

The CMS-BPLC template was fabricated by using chiral dopant R5011 (1.5 wt%), nematic liquid crystal BL002 (80.2 wt%), chiral mesogenic reactive monomer LC756 (1 wt%), mesogenic reactive monomer RM257 (9.4 wt%), and monomer TPGDA (7.4 wt%). The material R5011 possesses a right-handed helical twist power (HTP) of $126 \mu\text{m}^{-1}$ (from HCCH). The material BL002 is a room temperature nematic LC having the dielectric anisotropy ($\Delta\epsilon$) = 17.2, birefringence (Δn) = 0.2460, and nematic to isotropic transition temperature (T_{NI}) = 74°C . LC756 is a chiral mesogenic reactive monomer with diacrylate functionality and a right-handed HTP of $76 \mu\text{m}^{-1}$ (from Daken Chemicals, China). The monomer RM257 is an achiral mesogenic reactive monomer with diacrylate (from Merck). The material TPGDA is a diacrylate non-mesogenic monomer (from Sigma-Aldrich). To induce radical polymerization, a photo-initiator (Irgacure-651, 0.5 wt%, from Sigma-Aldrich) was added to the mixture. The molecular structures of

the materials are shown in Fig. 1. The monomer RM257 exhibits a nematic LC phase between 68.7°C and 128.2°C (Fig. S1). The material LC756 is a mesogenic chiral dopant comprising two acrylate functional groups in its structure. Also, it exhibits the nematic LC phase at temperatures ranging from 78.4°C to 90.3°C on heating and 84.8°C to 67.7°C on cooling (Fig. S2). Usually, higher monomer concentration is a prerequisite for this approach because the polymer network must be mechanically strong enough to retain its stability and periodicity. So, we judiciously choose the higher monomer concentration.

2.2. Methods

The experimental procedure for the fabrication of the CMS-BPLC template is shown in Fig. 2. First, the BPLC precursor is prepared by adding the appropriate weight percentages of materials and mixing thoroughly at 85°C , at which LC756 and RM257 exhibit the nematic LC phase. Then, the obtained homogeneous mixture was infiltrated into the experimental cell by capillary action at 85°C . The polarizing optical microscope (POM) (Nikon, Eclipse LV100POL) and the reflection spectrometer (USB4000, Ocean Optics) were used to characterize the BPLC. The temperature controller (Instec, MK2000) controls the temperature of the sample. The experimental in-plane switching (IPS) cell consists of comb-like interdigitated electrodes on the bottom substrate with each electrode width of $15 \mu\text{m}$ and separated by $15 \mu\text{m}$, with no electrodes on the top substrate. A diameter spacer of $20 \mu\text{m}$ was used to maintain a uniform cell gap between the top and bottom substrates. The details of the BPLC driving mechanism by IPS adapted by us can be found elsewhere [46,47]. The BPLC phase stabilization is carried out by irradiating ultraviolet light (peak wavelength of 365 nm) having an intensity of $20 \text{ mW}/\text{cm}^2$ for 15 min at a fixed temperature. Again, the CMS-BPLC phase range was characterized by POM and spectrometer.

Further, the LC, chiral dopant, and uncured monomer molecules are extracted by keeping the cell in a hexane-dichloromethane (80:20) solution for two days. After confirming that all the targeted molecules are washed out, the hexane-dichloromethane solution is evaporated, and the CMS-BPLC template is obtained. The microstructural characterizations were performed using field emission scanning electron microscopy (FESEM). In the final step, the same achiral nematic LC, BL002, is refilled into the template at 85°C and proceeded for structural and electro-optical characterization. Several experiments are performed for T-BPLC, including phase identification and electro-optics. The field-dependent transmittance was measured by a lab-made setup consisting of a He-Ne laser (wavelength = 632 nm) and a set of crossed polarizers. The transmitted intensity was read out by a photodiode connected to the oscilloscope (Tektronix, AFG3102). The incident polarization is set to 45° concerning the direction of the long IPS electrodes.

3. Results and discussion

3.1. Fabrication of CMS-BPLC

First, we examined the phases and subsequent temperature range of BPLC before phase stabilization. As depicted in Fig. 3a, the optical textures were covered by the green platelets and fewer red platelets in the BP II phase, whereas the red and yellow platelets appeared in the BP I phase. These Mosaic colors are Bragg reflections of cubic lattices those oriented parallel to the direction of light propagation. The phase transitions as observed: Iso 72.4°C BP II 70.3°C BP I 67.3°C Cholesteric liquid crystal (ChLC) (here, the Iso and ChLC refer to the temperature above the T_{NI} and the cholesteric phase, respectively), covering 2.1°C of the BP II phase followed by 3°C of BP I phase. The phase stabilization was performed at 69°C , corresponding to the BP I phase. As expected, the temperature range of CMS-BPLC is increased after phase stabilization. In this case, the BP phase appears at 72.4°C and extends up to 52.3°C . Fig. 3b depicts the BP range after phase stabilization. The

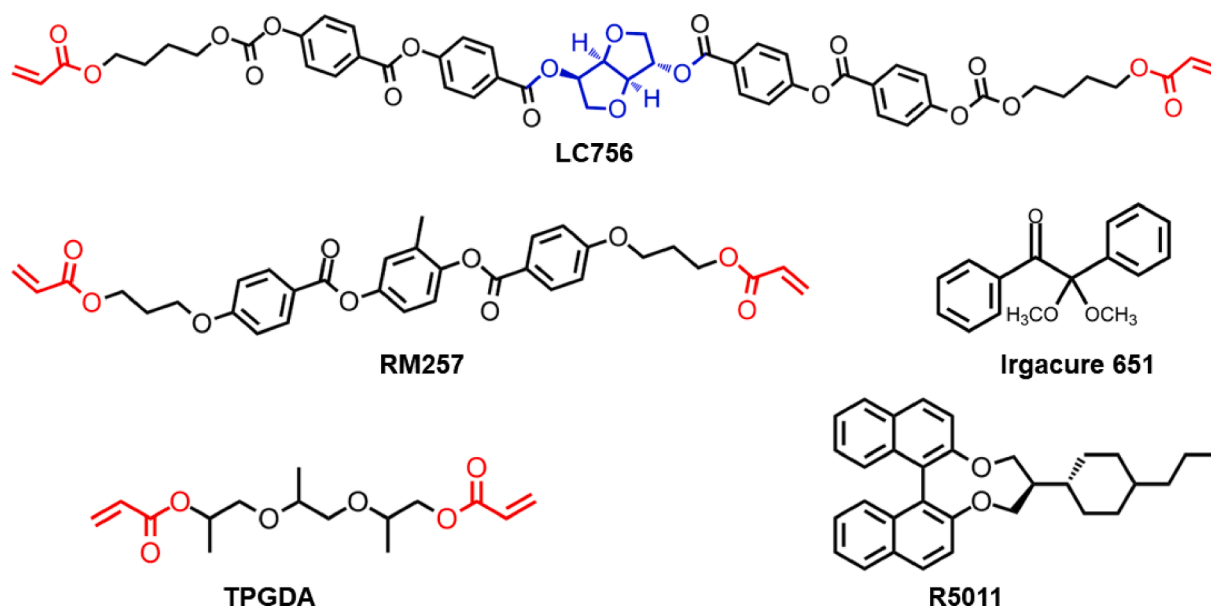


Fig. 1. Molecular structures of compounds used for fabricating CMS-BPLC template. The acrylate functional groups in the molecular structure are indicated as red color.

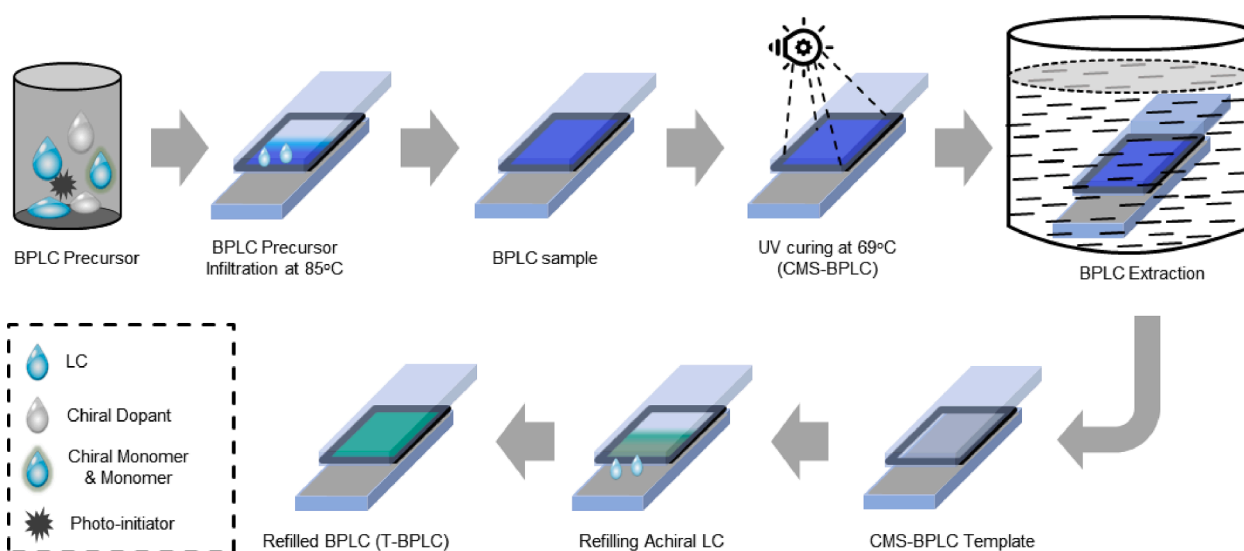


Fig. 2. Experimental procedure for making CMS-BPLC, CMS-BPLC template, and refilling achiral LC to produce T-BPLC. The refilling of the achiral nematic LC is performed at 85 °C.

sequence of phase transitions is denoted as Iso 72.4 °C BP II 67.8 °C BP I 52.3 °C ChLC. It shows 4.6 °C of BP II and 15.5 °C of BP I phase. Although the achieved phase range of BP II is not significant, comparatively, the BP I phase range has increased.

The Bragg reflection spectra were measured to estimate the reflection peaks associated with the optical textures. Due to the cubic crystalline structure, the central wavelength of the Bragg reflection is given by:

$$\lambda_B = \frac{2\bar{n}a}{\sqrt{h^2 + k^2 + l^2}} \quad (1)$$

where a is the lattice constant of BP cubic lattice, \bar{n} is the average refractive index ($\frac{2n_o + n_e}{3}$) of LC, and h, k, l are the Miller indices representing the orientation of the cubic lattice [48]. Therefore, the Bragg reflection is determined by the size of the cubic lattice, which is proportional to the pitch length (p), and the direction of the lattice

orientation. Moreover, the p is inversely proportional to the chiral dopant's concentration and HTP . For a given system, the p is the resultant of both chiral dopant and chiral monomer, and it can be expressed as:

$$p = \frac{1}{\sum_{i=1}^n HTP_i \times c_i} \quad (2)$$

where c_i is the concentration of both the chiral dopant and chiral monomer [27]. The calculated pitch of CMS-BPLC is found to be 377 nm.

The Bragg reflection spectra of CMS-BPLC are presented in Fig. 3c-d. Each peak in the reflection spectra is associated with a particular color in the POM image. In particular, before phase stabilization (Fig. 3c), two narrow bandwidth reflection peaks with λ_B of 562 nm and 632 nm for BP II originated from the reflections of (110) and (100) planes, respectively. Similarly, two reflection peaks of BP I, 613 nm and 630 nm, are from (200) and (110) planes, respectively. A short-range reflection

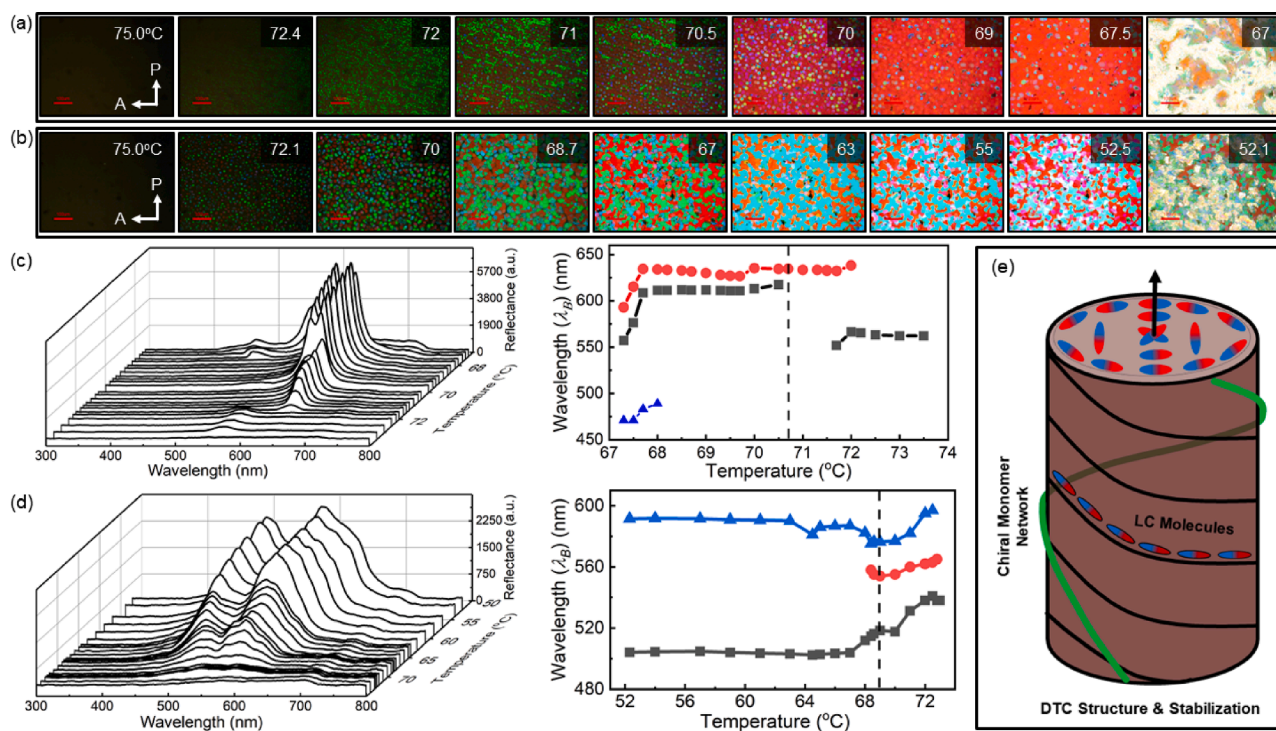


Fig. 3. The POM textures of CMS-BPLC: (a) Before, (b) After phase stabilization. The number on each image indicates the temperature. P: Polarizer; A: Analyzer. Measured Bragg reflection spectra for CMS-BPLC: (c) Before, (d) After phase stabilization. The dotted line indicates the phase transition between BP I and BP II. (e) Schematic representation of structural stability of DTC by chiral mesogenic monomers. CM: Chiral monomer.

(480 nm) emerged at the end of the BP I phase, which is expected to be from the (211) plane. Since the chiral monomer may not fully contribute to the DTC formation, a significant deviation exists in the estimation of λ_B . After the phase separation (Fig. 3d), λ_B is shifted towards smaller wavelengths and appeared at 538 nm, 597 nm, and 560 nm for BP II, while it appeared at 592 nm and 504 nm for BP I. Since the chiral monomer influence may exist even after polymerization, the reflections largely deviate from theoretical calculations. We presume that the chiral monomer is more likely to form a polymer network in both the disclination lines and inside the DTC, as depicted in Fig. 3e. The LC molecules may not lose their helicity due to polymer network formation, as the network surface may carry traces of BPLC orientation. The comparative study of pre- and post-polymerization optical textures and reflection measurements reveals no significant distortion to the self-assembly of DTCs and hence supports conjectures. The pitch of the polymer network formed inside the DTC may not be the same as that of the liquid crystal since there is a high possibility that the chiral monomer, under a strong helical twist, polymerizes with monomers even in the disclination lines. The bandwidth of the reflection peak significantly broadens after phase stabilization. The band's broadening may be associated with overlapping two close peaks.

3.2. Fabrication of CM-BPLC template

After necessary characterizations, the LC and uncured monomer molecules were extracted by immersing the sample into the hexane-dichloromethane solution and proceeded for further studies. The UV-visible spectra were measured at room temperature corresponding to the cholesteric phase to confirm the LC extraction (Fig. 4a). The sample shows no indication of transmission peak after LC extraction, so it confirms that all the LC molecules and chiral components are washed out during extraction. Therefore, only the polymer network is left over, and the targeted CMS-BPLC template can be realized. Further, we separated the top substrate and performed FESEM characterizations. Fig. 4b shows a microstructure image of a fabricated CMS-BPLC

template. The thickness of the network strand is smaller than 10 nm. The network density seems slightly higher than a conventional PS-BPLC template polymer network reported elsewhere [45]. This is thought to be due to the novel structural stability of DTC by chiral monomer [27]. The network shrinkage anticipated may not be significant during the LC extraction process because of the increased network structure density. The non-uniformity of the network density could have originated from the relatively less network formation inside the DTC.

3.3. T-BPLC and Electro-Optical properties

The same achiral nematic LC without chiral dopant and monomer is refilled into the prepared template for further studies. In refilling, we immersed the CMS-BPLC template into the LC and left the sample for a few days under a vacuum. Thus, the LC slowly infiltrates into the polymer network. The sample is ready for further characterization after a few heating cycles above T_{NI} .

We examined the sample with POM and recorded reflection spectra after refilling the achiral nematic LC into the CMS-BPLC template (Fig. 5a,b). Interestingly, the refilled achiral LC exhibits the BPLC phase in the CM-BPLC template (Fig. 5a). The achiral LC reconfigures the BP's orientational order through a spatially distributed CMS-BPLC template. These findings reveal that the chiral monomer network structure serves as the conventional BPLC template. This suggests that the surface memorized anchoring or pinning is strong enough to extend the surface orientation into the DTC bulk. In other words, the spatially distributed polymer network directs the LC molecules at their immediate vicinity to follow the BPLC traces recorded on the network surface, and this orientation extends into the bulk through elastic interaction. The coherence length is undoubtedly reduced due to structural stability. As a result, more LC molecules make direct contact with the polymer network, increasing the surface interaction strength. Therefore, the orientation of LC in the immediate vicinity of the network plays an essential role in the reconstruction of DTC. Subsequently, Bragg reflection measurements are performed, revealing that the cubic lattice

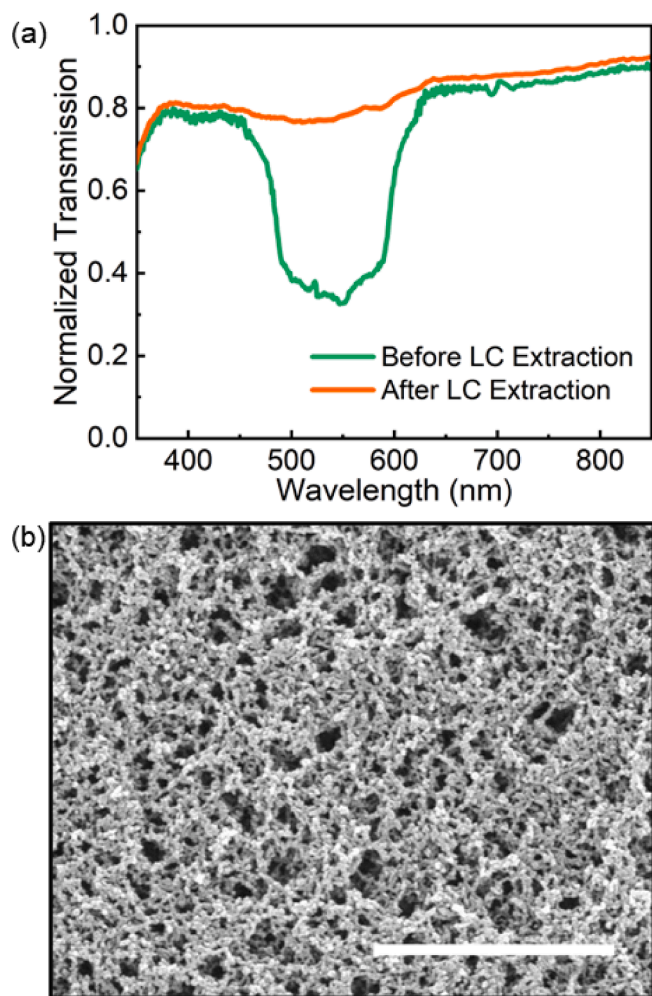


Fig. 4. (a) UV-visible spectra of the CMS-BPLC before and after BPLC extraction. (b) FESEM micrograph of CMS-BPLC template. The scale bar is 2 μm .

structure can be reconstructed using achiral LC (Fig. 5b). Although the T-BPLC analogs the monodomain-like optical textures, several smaller platelets with distinct boundaries can be seen in the magnified optical image. The platelets are relatively smaller in size than those of the conventional PS-BPLC. In addition, the measured Bragg reflection spectra correlate with POM texture (Fig. 5b,c). For T-BPLC, the temperature-independent λ_B of 490 nm with a bandwidth of 90 ± 5 nm is achieved. The obtained bandwidth remains constant throughout the spectra (Fig. S3). It may be noted that no phase transitions were observed compared to the pure LC in the template system. However, the total phase range of 42.9°C was achieved, including near ambient temperature (28.2°C) on cooling. It demonstrates that LC molecules mimic the orientation of pre-polymerized BPLC in a densely packed polymer network. Interestingly, this system also exhibits the ChLC phase on a further temperature decrease (Fig. S4). The surface anchoring of the polymer network within the DTC plays a crucial role in T-BPLC. The phase exhibits a slightly wider bandwidth, which is a characteristic of the T-BPLC. These Bragg reflections can be originated from the cubic structure of T-BPLC. The reflection peak of T-BPLC lies within the band of CMS-BPLC.

The electro-optics of both CMS-BPLC and T-BPLC are measured at 56°C , as shown in Fig. 5d-f. A wave function generator (Tektronix AFG31000) and amplifier (FLC Electronics) delivered a square wave voltage to the sample at 1 kHz. The switching of T-BPLC also exhibits a change in the birefringence (Fig. 5d). Assuming that the network topology remains unchanged under strong fields, the change in

birefringence is due solely to the reorientation of LC molecules. The field-dependent transmittance curves of T-BPLC exhibit drastic changes compared to CMS-BPLC (Fig. 5e). Both threshold field E_{th} (10 % transmission) and operating field E_{op} (90 % transmission) of T-BPLC are decreased by more than half of the CMS-BPLC. In particular, the measured E_{th} is $1.5\text{ V}/\mu\text{m}$ and $0.8\text{ V}/\mu\text{m}$, and E_{op} is $6.5\text{ V}/\mu\text{m}$ and $3.1\text{ V}/\mu\text{m}$ for CMS-BPLC and T-BPLC, respectively. Such a substantial decrease in E_{th} and E_{op} could be attributed to LC molecules reorienting along the field direction rather than the unwinding of twisted cylindrical self-assembly. It is worth noting that the T-BPLC has a comparatively high Kerr constant (K) ($4.1\text{ nm}/\text{V}^2$), whereas the CMS-BPLC exhibits a low Kerr value ($0.7\text{ nm}/\text{V}^2$) (Fig. S5). Perhaps the absence of chiral additives results in an increase in the Kerr constant in the system. Furthermore, the absence of undesired chiral dopants and uncured monomer molecules not participating in the electro-optical effect is expected to enhance the system's purity. This could be another reason for the increase in the K . The K is directly proportional to the Δn , $\Delta\epsilon$, and p . The increase of K is relatively 5 times higher than CMS-BPLC, which is substantially higher.

The measured response times of refilled LC are also comparable to CMS-BPLC (Fig. 5f). The rise and decay response times are defined as 10 % and 90 % transmission change upon field-on and field-off, respectively. Interestingly, fast rise time and slow decay time were achieved for refilled BPLC compared to CMS-BPLC. The rise time is 2.6 ms and 0.8 ms, and the decay time is 1 ms and 2.6 ms for CMS-BPLC and T-BPLC, respectively. The difference in the switching response time is expected to originate from the difference in the elastic constant of these two materials [49,50]. This indicates that the relaxation duration is governed by the combined effect of the elastic energy of nematic LC and the surface interaction/pinning energy imposed by the spatially distributed polymer network (Supplementary Section 3). On the other hand, the greater surface memorized pinning effect caused by larger polymer network density is a critical characteristic in this system.

In a current approach, the dispersed chiral monomer occupies inside the DTC along with topological disclination lines at which a dense and completely new template can be realized after polymerization. The reconstruction of highly twisted DTC structures by achiral LC in T-BPLC is directed by the spatial periodicity of the polymer template with director traces on the surface. Our proposed T-BPLC also possesses a low E_{th} and E_{op} . This unusual behavior originates from the absence of chiral molecules, which necessitates an additional electric torque to unwind the DTC and reorient it along the field direction. The only weak coupling interaction between achiral LC molecules and polymer network reduces E_{op} to half that of the conventional polymer stabilized BPLC. Therefore, this device can be driven with traditional active-matrix circuits such as TFTs. Furthermore, eliminating chiral molecules in a BPLC phase is also advantageous to obtain a sub-millisecond response time in the system. This unique feature of the proposed BPLC system offers several benefits, including easy implementation to real-world device applications. On the other hand, the increased surface pinning effect due to higher polymer network density is a key parameter in this system. In this aspect, a deeper understanding of the system from a more theoretical perspective is required.

4. Conclusions

We have demonstrated a new CMS-BPLC-based template, which overcomes the fundamental challenges of BPLC, including shorter phase ranges and high driving fields. The CMS-BPLC offers a more robust template for achiral LC to induce a BPLC phase that remains stable over 42°C due to the improved structural stability. In our system, the driving field is reduced by 52 % while the superior electro-optical properties are retained. Our system's high stability and outstanding electro-optics make it simple to integrate into any TFT driving circuit.

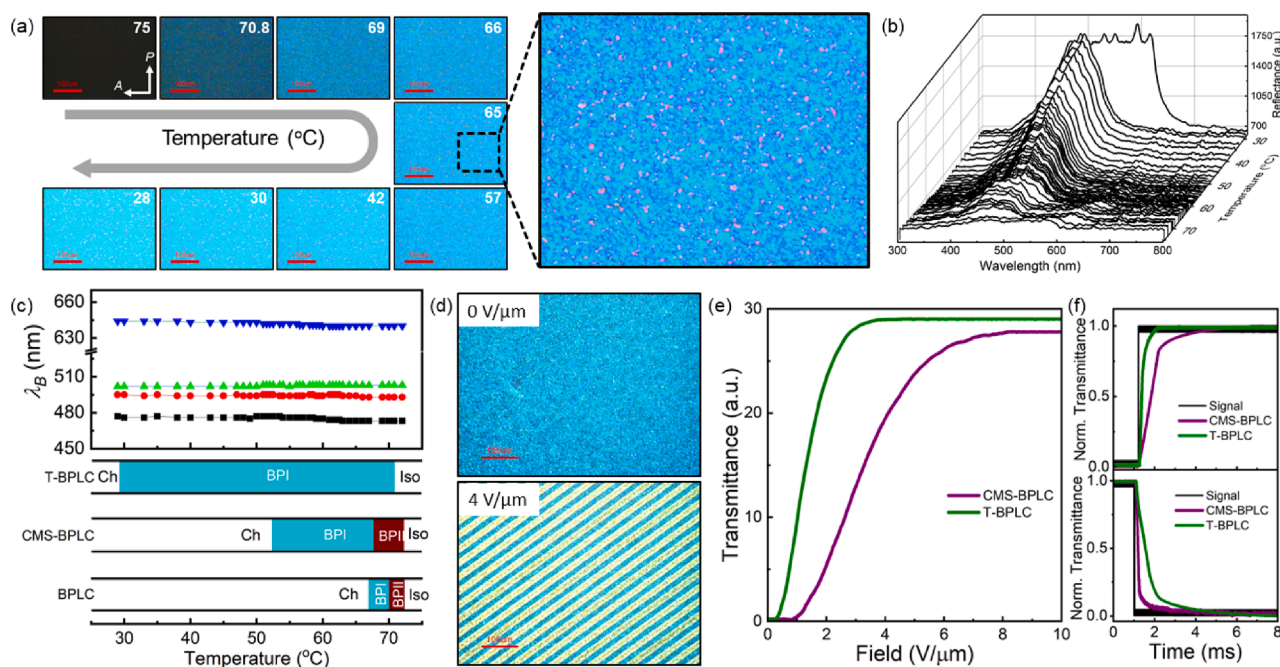


Fig. 5. (a) POM textures of the sample after refilling achiral LC. The number on each image indicates temperature. (b) Bragg reflection spectra of T-BPLC. The broad reflection peak at the end of the spectra corresponds to the ChLC phase. (c) The center wavelength of the reflection peak (λ_B) as a function of temperature and the relative phase range of CMS-BPLC and T-BPLC. Ch: Cholesteric LC phase; Iso: Isotropic phase. (d) Switching of T-BPLC. (e) Field-dependent transmittance of CMS-BPLC and T-BPLC was measured at 56 °C. (f) Rise and decay response time of CMS-BPLC and T-BPLC.

CRediT authorship contribution statement

Srinivas Pagidi: Conceptualization, Investigation, Methodology, Writing – original draft. **Ramesh Manda:** Conceptualization, Funding acquisition, Investigation, Methodology, Supervision, Writing – original draft. **Sujaya Kumar Vishwanath:** Methodology, Validation. **Moon-Young Choi:** Data curation, Validation. **Mohsin Hassan Saeed:** Data curation, Validation. **Surajit Dhara:** Data curation, Validation. **Jun-Hee Na.:** Funding acquisition, Investigation, Supervision, Writing – review & editing.

Declaration of competing interest

The authors declare that they have no known competing financial interests or personal relationships that could have appeared to influence the work reported in this paper.

Data availability

No data was used for the research described in the article.

Acknowledgements

This work is supported by the Ramanujan Fellowship (RJF/2022/000094), Science and Engineering Research Board (SERB), India. Also funded by the National Research Foundation of Korea (NRF) grant funded by the Korean Government (MSIT) (No. 2021R1A4A1032762).

Appendix A. Supplementary data

Supplementary data to this article can be found online at <https://doi.org/10.1016/j.molliq.2024.124311>.

References

- [1] Y. Yang, L. Wang, H. Yang, Q. Li, 3D chiral photonic nanostructures based on blue-phase liquid crystals, *Small Sci.* 1 (6) (2021) 2100007.

- [2] M.J. Lee, C.H. Chang, W. Lee, Label-free protein sensing by employing blue phase liquid crystal. *Biomed. Opt. Express.* 8 (3) (2017) 1712–1720.
- [3] B. Gurboga, E. Kemiklioglu, Optical sensing of organic vapor using blue phase liquid crystals, *Liq. Cryst.* 49 (11) (2022) 1428–1435.
- [4] R. Manda, S. Pagidi, Y. Heo, Y.J. Lim, M. Kim, S.H. Lee, Electrically tunable photonic band gap structure in monodomain blue-phase liquid crystals, *NPG Asia Mater.* 12 (1) (2020) 42.
- [5] R. Manda, S. Pagidi, Y. Heo, S.S. Hoon, H.G. Lee, H.S. Park, D. Mun, Y.J. Lim, S. H. Lee, P-146: Electrically tunable bandpass filter with narrow bandwidth of 27 nm, *SID Symposium Digest of Technical Papers.* 51 (1) (2020) 1930–1933.
- [6] R. Manda, S. Pagidi, Y.J. Heo, Y.J. Lim, M.S. Kim, S.H. Lee, Polymer-stabilized monodomain blue phase diffraction grating, *Adv. Mater. Interfaces.* 7 (9) (2020) 1901923.
- [7] H. Kikuchi, *Liquid crystalline blue phases*, Springer, Berlin, Heidelberg, In *Liquid crystalline functional assemblies and their supramolecular structures*, 2008, pp. 99–117.
- [8] S. Cho, M. Ozaki, Blue phase liquid crystals with tailored crystal orientation for photonic applications, *Symmetry.* 13 (9) (2021) 1584.
- [9] J. Yan, L. Rao, M. Jiao, Y. Li, C.H. Cheng, S.T. Wu, Polymer-stabilized optically isotropic liquid crystals for next-generation display and photonics applications, *J. Mater. Chem.* 21 (22) (2011) 7870–7877.
- [10] J. Yan, H.C. Cheng, S. Gauza, Y. Li, M. Jiao, L. Rao, S.T. Wu, Extended Kerr effect of polymer-stabilized blue-phase liquid crystals, *Appl. Phys. Lett.* 96 (7) (2010) 071105.
- [11] M. Lopez-García, N. Masters, H.E. O'Brien, J. Lennon, G. Atkinson, M.J. Cryan, R. Oulton, H.M. Whitney, Light-induced dynamic structural color by intracellular 3D photonic crystals in brown algae, *Sci. Adv.* 4 (4) (2018) eaan8917.
- [12] Y. Wang, H. Cui, Q. Zhao, X. Du, Chameleon-Inspired Structural-Color Actuators, *Matter* 1 (3) (2019) 626–638.
- [13] H. Kikuchi, M. Yokota, Y. Hisakado, H. Yang, T. Kajiyama, Polymer-stabilized liquid crystal blue phases, *Nat. Mater.* 1 (1) (2002) 64–68.
- [14] A.P. Draude, T.Y. Kalavalapalli, M. Iliut, B. McConnell, I. Dierking, Stabilization of liquid crystal blue phases by carbon nanoparticles of varying dimensionality, *Nanoscale Adv.* 2 (6) (2020) 2404–2409.
- [15] L. Wang, W. He, Q. Wang, M. Yu, X. Xiao, Y. Zhang, M. Ellahi, D. Zhao, H. Yang, L. Guo, Polymer-stabilized nanoparticle-enriched blue phase liquid crystals, *J. Mater. Chem. C.* 1 (40) (2013) 6526–6531.
- [16] W. Hu, L. Wang, M. Wang, T. Zhong, Q. Wang, L. Zhang, F. Chen, K. Li, Z. Miao, D. Yang, H. Yang, Ultrastable liquid crystalline blue phase from molecular synergistic self-assembly, *Nat. Commun.* 12 (1) (2021) 1440.
- [17] J. Liu, W. Liu, B. Guan, B. Wang, L. Shi, F. Jin, Z. Zheng, J. Wang, T. Ikeda, L. Jiang, Diffusionless transformation of soft cubic superstructure from amorphous to simple cubic and body-centered cubic phases, *Nat. Commun.* 12 (1) (2021) 3477.
- [18] Z. Zheng, D. Shen, P. Huang, Wide blue phase range of chiral nematic liquid crystal doped with bent-shaped molecules, *New J. Phys.* 12 (11) (2010) 113018.
- [19] V. Punjani, G. Mohiuddin, S. Kaur, A.R. Choudhury, S. Paladugu, S. Dhara, S. Ghosh, S.K. Pal, Chiral bent-shaped molecules exhibiting unusually wide range

- of blue liquid-crystalline phases and multistimuli-responsive behavior, *Chem. Eur. J.* 26 (26) (2020) 5859–5871.
- [20] W. He, G. Pan, Z. Yang, D. Zhao, G. Niu, W. Huang, X. Yuan, J. Guo, H. Cao, H. Yang, Wide blue phase range in a hydrogen-bonded self-assembled complex of chiral fluoro-substituted benzoic acid and pyridine derivative, *Adv. Mater.* 21 (20) (2009) 2050–2053.
- [21] A. Yoshizawa, M. Sato, J. Rokunohe, A blue phase observed for a novel chiral compound possessing molecular biaxiality, *J. Mater. Chem.* 15 (32) (2005) 3285–3290.
- [22] J. Tang, F. Liu, M. Lu, D. Zhao, InP/ZnS quantum dots doped blue phase liquid crystal with wide temperature range and low driving voltage, *Sci. Rep.* 10 (1) (2020) 18067.
- [23] S. Yabu, Y. Tanaka, K. Tagashira, H. Yoshida, A. Fujii, H. Kikuchi, M. Ozaki, Polarization-independent refractive index tuning using gold nanoparticle-stabilized blue phase liquid crystals, *Opt. Lett.* 36 (18) (2011) 3578–3580.
- [24] P. Li, X.Q. Wang, D. Shen, Z.G. Zheng, A long-term stable low-viscous self-organized blue phase liquid crystal superstructure with wide operation temperature range, *Liq. Cryst.* 49 (2) (2022) 192–200.
- [25] Y. Huang, H. Chen, G. Tan, H. Tobata, S.I. Yamamoto, E. Okabe, Y.F. Lan, C.Y. Tsai, S.T. Wu, Optimized blue-phase liquid crystal for field-sequential-color displays, *Opt. Mater. Express* 7 (2) (2017) 641–650.
- [26] L. Rao, Z. Ge, S.T. Wu, S.H. Lee, Low voltage blue-phase liquid crystal displays, *App. Phys. Lett.* 95 (23) (2009) 231101.
- [27] R. Manda, M.S. Kim, E. Jeong Shin, M.S. Gong, G. Murali, K. Sandeep, M.H. Lee, J. H. Lee, S.H. Lee, Phase stabilisation of blue-phase liquid crystals using a polymerisable chiral additive, *Liq. Cryst.* 44 (6) (2017) 1059–1068.
- [28] R. Manda, S. Pagidi, S.S. Bhattacharya, H. Yoo, A. Kumar, Y.J. Lim, S.H. Lee, Ultra-fast switching blue phase liquid crystals diffraction grating stabilized by chiral monomer, *J. Phys. D Appl. Phys.* 51 (18) (2018) 185103.
- [29] Y. Feng, Z. Zhu, H. Zhang, K. Huang, T. Huang, W.M. Han, D.Q. Wu, J. Lu, Chiral polymer network stabilised blue phase liquid crystals, *Liq. Cryst.* 47 (14–15) (2020) 2184–2193.
- [30] H. Furue, W. Neyatani, S. Igari, Y. Kogo, Study on blue phase liquid crystals using photocurable monomers for nano-structured materials, *Ferroelectrics* 495 (2) (2016) 150–157.
- [31] J. Yang, W. Zhao, Z. Yang, W. He, J. Wang, T. Ikeda, L. Jiang, Photonic shape memory polymer based on liquid crystalline blue phase films, *ACS Appl. Mater. Interfaces* 11 (49) (2019) 46124–46131.
- [32] F. Castles, F.V. Day, S.M. Morris, D.H. Ko, D.J. Gardiner, M.M. Qasim, S. Nosheen, P.J.W. Hands, S.S. Choi, R.H. Friend, H.J. Coles, Blue-phase templated fabrication of three-dimensional nanostructures for photonic applications, *Nat. Mater.* 11 (7) (2012) 599–603.
- [33] M. Ravník, J.I. Fukuda, Templated blue phases, *Soft Mater.* 11 (43) (2015) 8417–8425.
- [34] M. Wang, C. Zou, J. Sun, L. Zhang, L. Wang, J. Xiao, F. Li, P. Song, H. Yang, Asymmetric tunable photonic bandgaps in self-organized 3D nanostructure of polymer-stabilized blue phase I modulated by voltage polarity, *Adv. Funct. Mater.* 27 (46) (2017) 1702261.
- [35] D.C. Hu, W.H. Li, X.W. Chen, X.L. Ma, Y.J. Lee, J.G. Lu, Template effect on reconstruction of blue phase liquid crystal, *J. Soc. Information Disp.* 24 (10) (2016) 593–599.
- [36] X.W. Xu, Y.J. Liu, F. Wang, D. Luo, Narrow linewidth and temperature insensitive blue phase liquid crystal films, *IEEE Photonics J.* 10 (6) (2018) 1–7.
- [37] S.S. Choi, S.M. Morris, W.T. Huck, H.J. Coles, Simultaneous red–green–blue reflection and wavelength tuning from an achiral liquid crystal and a polymer template, *Adv. Mater.* 22 (1) (2010) 53–56.
- [38] H. Coles, S. Morris, Liquid-crystal lasers, *Nat. Photon.* 4 (10) (2010) 676–685.
- [39] X. Xu, Z. Liu, Y. Liu, X. Zhang, Z. Zheng, D. Luo, X. Sun, Electrically switchable, hyper-reflective blue phase liquid crystals films, *Adv. Opt. Mater.* 6 (3) (2018) 1700891.
- [40] S. Zha, H. Zhang, C. Sun, Y. Feng, J. Lu, Multi-Wavelength filters of templated blue phase liquid crystal, *Cryst.* 9 (9) (2019) 451.
- [41] A. Jákli, G.G. Nair, C.K. Lee, R. Sun, L.C. Chien, Macroscopic chirality of a liquid crystal from nonchiral molecules, *Phys. Rev. E* 63 (6) (2001) 061710.
- [42] D. Zhang, W. Shi, H. Cao, Y. Chen, L. Zhao, P. Gan, Z. Yang, D. Wang, W. He, Reflective band memory effect of cholesteric polymer networks based on washout/refilling method, *Macromol. Chem. Phys.* 221 (22) (2020) 1900572.
- [43] T. Huang, J. Lu, 12.3: Multi-phase and multi-pitch twist structure liquid crystals with polymer template, *SID Symposium Digest of Technical Papers* 52 (1) (2021) 82–85.
- [44] V.P. Panov, S.P. Sreenilayam, Y.P. Panarin, J.K. Vij, C.J. Welch, G.H. Mehl, Characterization of the submicrometer hierarchy levels in the twist-bend nematic phase with nanometric helices via photopolymerization, Explanation for the Sign Reversal in the Polar Response, *Nano Lett.* 17 (12) (2017) 7515–7519.
- [45] H.C. Jau, W.M. Lai, C.W. Chen, Y.T. Lin, H.K. Hsu, C.H. Chen, C.C. Wang, T.H. Lin, Study of electro-optical properties of templated blue phase liquid crystals, *Opt. Mater. Express* 3 (9) (2013) 1516–1522.
- [46] H. Hong, H. Shin, I. Chung, In-plane switching technology for liquid crystal display television, *J. Disp. Techn.* 3 (4) (2007) 361–370.
- [47] D.H. Kim, Y.J. Lim, D.E. Kim, H. Ren, S.H. Ahn, S.H. Lee, Past, present, and future of fringe-field switching-liquid crystal display, *J. Information Disp.* 15 (2) (2014) 99–106.
- [48] E. Otón, H. Yoshida, P. Morawick, O. Strzeżysz, P. Kula, M. Ozaki, W. Piecek, Orientation control of ideal blue phase photonic crystals, *Sci. Rep.* 10 (1) (2020) 10148.
- [49] S.S. Hu, J.J. Wu, C.C. Hsu, T.J. Chen, K.L. Lee, Simulation of the in-plane-switching blue-phase liquid crystal using the director model, *Opt. Express* 20 (21) (2012) 23954–23959.
- [50] P.R. Gerber, Electro-optical effects of a small-pitch blue-phase system, *Mol. Cryst. Liq. Cryst.* 116 (3–4) (1985) 197–206.